PNAS
www.pnas.org

Supplementary Information for

PROTEASE-ACTIVATED RECEPTOR-2 IN ENDOSOMES SIGNALS PERSISTENT PAIN OF IRRITABLE BOWEL SYNDROME

Nestor N. Jimenez-Vargas, Luke A. Pattison, Peishen Zhao, TinaMarie Lieu, Rocco Latorre, Dane D. Jensen, Joel Castro, Luigi Aurelio, Giang T. Le, Bernard Flynn, Carmen Klein Herenbrink, Holly R. Yeatman, Laura Edgington-Mitchell, Christopher J.H. Porter, Michelle L. Halls, Meritxell Canals, Nicholas A. Veldhuis, Daniel P. Poole, Peter McLean, Gareth A. Hicks, Nicole Scheff, Elyssa Chen, Aditi Bhattacharya, Brian L. Schmidt, Stuart M. Brierley, Stephen J. Vanner, Nigel W. Bunnett

Corresponding Author: Nigel W. Bunnett, Ph.D., Columbia University College of Physicians and Surgeons, 21 Audubon Avenue, Rm 209, New York City, New York 10032, USA
Email: nb33@cumc.columbia.edu

This PDF file includes:

Supplementary text
Figs. S1 to S11
Captions for movies S1 to S2
References for SI reference citations

Other supplementary materials for this manuscript include the following:

Movies S1 to S2

www.pnas.org/cgi/doi/10.1073/pnas.1721891115

Supplementary Information Text

Methods

Human biopsy samples. The Queen's University Human Ethics Committee approved human studies. All subjects gave informed consent. Endoscopic biopsies were obtained from the descending colon of 13 adult IBS-D patients (12 female) diagnosed using ROME III criteria for diarrhea-predominant IBS and of 12 healthy controls. All IBS patients had symptoms greater than 1 year and most were greater than 5 years. Celiac disease was excluded by blood test and patients over 40 years with daily diarrhea were biopsied at the time of colonoscopy to exclude microscopic colitis. None of the patients had a history suggestive of post-infectious IBS. Control biopsies were obtained from patients undergoing colon screening who did not have gastrointestinal symptoms. Biopsies (8 samples per patient) were incubated in 250 µl of RPMI medium containing 10% fetal calf serum, penicillin/streptomycin and gentamicin/amphotericin B (95%O_2/5%CO_2, 24 h, 37°C) (1). Supernatants were stored at -80°C. Supernatants from 4-6 patients were pooled and studied in individual experiments.

Animals. Institutional Animal Care and Use Committees of Queen's University, Monash University, Flinders University, New York University, and the South Australian Health and Medical Research Institute approved all studies. Mice (C57BL/6, males, 6-15 weeks) and rats (Sprague-Dawley, males, 8-12 weeks) were studied. Animals were maintained in a temperature-controlled environment with a 12 h light/dark cycle and free access to food and water. Animals were killed by CO_2 inhalation or anesthetic overdose and thoracotomy. Animals were randomized for treatments and no animals were excluded from studies.

***Par_2-$Na_V1.8$* mice.** *F2rl1* conditional knock-out C57BL/6 mice were generated by genOway (Lyon, France). The last exon of *F2rl1*, encoding for the transmembrane, extracellular and cytoplasmic domains of F2RL1, was flanked by *lox*P sites and a neomycin cassette in intron 1. The neomycin cassette was excised by breeding these mice with a C57BL/6 Flp-expressing mouse line. To delete *Par_2* in peripheral neurons, *F2rl1* conditional knock-out mice were bred with mice expressing Cre recombinase under the control of the *Scn10a* gene promoter (B6.129-Scn10a$^{tm2(cre)Jnw/H}$) (2). Deletion of PAR_2 in $Na_V1.8$ nociceptors was evaluated by immunofluorescence. DRG from wild-type and *Par_2-$Na_V1.8$* mice were fixed in 10% formalin for 3 h, transferred to 70% alcohol, and embedded in paraffin. Sections (5 µm) were deparaffinized, rehydrated, microwaved in sodium citrate buffer, washed, and then blocked in SuperBlock™ (ThermoFisher Scientific) for one hour at room temperature. Sections were incubated with mouse antibody to PAR_2 conjugated to Alexa-488 (Santa Cruz Biotechnology, SC-13504, 1:200, 4°C, overnight), and with guinea pig antibody to $Na_V1.8$ (Alomone Labs, AGP-029, 1:200, 4°C, overnight), followed by goat anti-guinea pig secondary antibody conjugated to Alexa Fluor-594 (Life Technologies, A11076, 1:500, room temperature, 1 hour). Sections were imaged with a Nikon Eclipse Ti microscope using 10x magnification; images were captured with a Photometrics CoolSNAP camera.

Somatic nociception and inflammation. Mice were acclimatized to the experimental apparatus, room and investigator for 1-2 h on 2 successive days before studies. Investigators were blinded to the test agents. Mice were sedated (5% isoflurane) for intraplantar injections. Dy4a, Dy4 inact, PS2, PS2 inact (all 50 µM) or vehicle (0.2% DMSO in 0.9% NaCl) (10 µl) was injected into the left hindpaw. After 30 min, trypsin (10 or 80 nM), CS (2.5 or 5 µM) or NE (1.2 or 3.9 µM) (all 10

µl) was injected into the same hindpaw. Mechanical nociceptive responses were evaluated by examining paw withdrawal to stimulation of the plantar surface of the hind-paw with calibrated von Frey filaments (VFF) (3). VFF scores were measured in triplicate to establish a baseline for each animal on the day before experiments, and were then measured for up to 4 h after protease administration. To assess edema, paw thickness was measured at the site of injection between the plantar and the dorsal surfaces of the paw using digital calipers. For evaluation of neutrophil infiltration, paws were collected at 4 h after intraplantar injection of trypsin (10 µl, 80 nM) or vehicle, fixed in 10% neutral buffered formalin for 48-72 h, bisected, and fixed in formalin for an additional 12 h. Tissue was decalcified in 10% 0.5 M EDTA for 6 days, washed in water, transferred to 70% ethanol for 24 h, and embedded in paraffin. Sections (5 µm) were incubated with neutrophil antibody Ly6G/6C clone NIMP-R14 (Abcam # ab2557, Lot # GR135037-1, AB_303154, 1:800, room temperature, 12 h). Sections were processed for chromogenic immunohistochemistry on a Ventana Medical Systems Discovery XT platform with online deparaffinization using Ventana's reagents. Ly6G/Ly6c was enzymatically treated with protease-3 (Ventana Medical Systems) for 8 min. Ly6G/Ly6c was detected with goat anti-rat horseradish peroxidase conjugated multimer incubated for 16 min.

Dissociation of DRG neurons for electrophysiological studies. DRG innervating the colon (T9-T13) were collected from C57BL/6 mice. Ganglia were digested by incubation in collagenase IV (1 mg/ml, Worthington) and dispase (4 mg/ml, Roche) (10 min, 37°C). DRG were triturated with a fire-polished Pasteur pipette, and further digested (5 min, 37°C). Neurons were washed, plated onto laminin- (0.017 mg/ml) and poly-D-lysine- (2 mg/ml) coated glass coverslips, and were maintained in F12 medium containing 10% fetal calf serum, penicillin and streptomycin (95% air, 5% CO_2, 16 h, 37ºC) until retrieval for electrophysiological studies.

Patch clamp recording. Small-diameter (<30 pF capacitance) neurons were studied because they display characteristics of nociceptors (1). Changes in excitability were quantified by measuring rheobase. Whole-cell perforated patch-clamp recordings were made using Amphotericin B (240 µg/ml, Sigma Aldrich) in current clamp mode at room temperature. The recording chamber was perfused with external solution at 2 ml/min. Recordings were made using Multiclamp 700B or Axopatch 200B amplifiers, digitized by Digidata 1440A or 1322A, and processed using pClamp 10.1 software (Molecular Devices). Solutions had the composition (mM): pipette - K-gluconate 110, KCl 30, HEPES 10, $MgCl_2$ 1, $CaCl_2$ 2; pH 7.25 with 1 M KOH; external - NaCl 140, KCl 5 HEPES 10, glucose 10, $MgCl_2$ 1, $CaCl_2$ 2; pH to 7.3-7.4 with 3 M NaOH. Neurons were preincubated with supernatants of colonic mucosal biopsies from HC or IBS-D subjects (200 µl supernatant were combined with 500 µl of F12 medium, filtered) for 30 min. Neurons were also preincubated with trypsin (50 nM, 10 min), NE (390 nM, 30 min), CS (500 nM, 60 min), thrombin (50 nM, 20 min), or vehicle (37°C), and washed. Rheobase was measured at T 0 or T 30 min after washing. To investigate mechanisms of protease-evoked effects, neurons were incubated with I-343 (100 nM, 300 nM, 10 µM, 30 min preincubation), SCH79797 (1 µM, 10 min), Dy4 (30 µM, 30 min), PS2 (15 µM, 30 min), PD98059 (50 µM, 30 min), GF109203X (10 µM, 30 min), or vehicle (preincubation and inclusion throughout). In experiments using the tripartite antagonist, neurons were preincubated with MIPS15479 (30 µM, 60 min, 37°C) or vehicle and washed. They were recovered in F12 medium at 37°C for variable times, challenged with HC or IBS-D supernatant or trypsin (50 nM, 10 min), and washed. Rheobase was measured 0 or 30 min after washing. In all experiments, the mean rheobase was calculated for neurons exposed to supernatants, proteases or vehicle.

Colonic afferent recordings. The colon and rectum (5-6 cm) was removed from C57BL/6 mice.

Afferent recordings were made from splanchnic nerves, as described (4, 5). Briefly, the intestine was opened and pinned flat, mucosal side up, in an organ bath. Tissue was superfused with a modified Krebs solution (mM: 117.9 NaCl, 4.7 KCl, 25 $NaHCO_3$, 1.3 NaH_2PO_4, 1.2 $MgSO_4$ $(H_2O)_7$, 2.5 $CaCl_2$, 11.1 D-glucose; 95% O_2, 5% CO_2, 34°C), containing the L-type calcium channel antagonist nifedipine (1 μM) to suppress smooth muscle activity, and the cyclooxygenase inhibitor indomethacin (3 μM) to suppress inhibitory actions of prostaglandins. The splanchnic nerve was extended into a paraffin-filled recording compartment, in which finely dissected strands were laid onto a platinum electrode for single-unit extracellular recordings of action potentials generated by mechanical stimulation of receptive fields in the colon. Receptive fields were identified by mechanical stimulation of the mucosal surface with a brush of sufficient stiffness to activate all types of mechanosensitive afferents. Once identified, receptive fields were tested with three distinct mechanical stimuli to enable classification: static probing with calibrated VFF (2 g force; 3 times for 3 sec), mucosal stroking with VFF (10 mg force; 10 times), or circular stretch (5 g; 1 min) (4, 5). Colonic nociceptors displayed high-mechanical activation thresholds and responded to noxious distension (40 mmHg), circular stretch (≥7g) or 2 g filament probing, but not to fine mucosal stroking (10 mg filament). These neurons express an array of channels and receptors involved in pain, become mechanically hypersensitive in models of chronic visceral pain, and have a nociceptor phenotype (4, 5). In the current study, they are therefore referred to as "colonic nociceptors". Once baseline colonic nociceptor responses to mechanical stimuli (2 g filament) had been established, mechanosensitivity was re-tested after 10 min application of trypsin (10 nM), NE (100 nM) or CS (100 nM). Proteases were applied to a metal cylinder placed over the receptive mucosal field of interest. This route of administration has been shown to activate colonic afferents (5). Action potentials were analyzed using the Spike 2 wavemark function and discriminated as single units on the basis of distinguishable waveform, amplitude and duration.

Colonic visceral hypersensitivity. Post-inflammatory hypersensitivity was induced by intracolonic administration of trinitrobenzene sulphonic acid (TNBS), as described (4, 5). Briefly, 12 week old mice were fasted overnight with access to 5% glucose solution. TNBS (100 μl, containing 4 mg TNBS in 30% EtOH) was administered to sedated mice (5% isoflurane) through a polyethylene catheter inserted 3 cm past the anus. Mice were then allowed to recover for 28 days. At this time, mice display colonic mechanical hypersensitivity, allodynia and hyperalgesia (4, 5).

Visceromotor Responses (VMR) to Colorectal Distension (CRD). Electromyography (EMG) of abdominal muscles was used to monitor VMR to CRD (6). Electrodes were implanted into the right abdominal muscle of mice under isoflurane anesthesia. Mice were recovered for at least three days before assessment of VMR. On the day of VMR assessment, mice were sedated with isoflurane, and vehicle (saline) or protease cocktail (10 nM trypsin, 100 nM NE, 100 nM CS) (100 μl) was administered into the colon *via* enema. In one group of mice, I-343 (30 mg/kg, 100 μl) was administered into the colon 30 min before the protease cocktail. A lubricated balloon (2.5 cm) was introduced into the colorectum to 0.25 cm past the anus. The balloon catheter was secured to the base of the tail and connected to a barostat (Isobar 3, G&J Electronics) for graded and pressure-controlled balloon distension. Mice were allowed to recover from anesthesia for 15 min before the CRD sequence. Distensions were applied at 20, 40, 50, 60, 70 and 80 mm Hg (20 s duration) at 4 min-intervals; the final distension was 30 min after administration of protease or vehicle. The EMG signal was recorded (NL100AK headstage), amplified (NL104), filtered (NL 125/126, Neurolog, Digitimer Ltd, bandpass 50–5000 Hz), and digitized (CED 1401, Cambridge Electronic Design) for off-line analysis using Spike2 (Cambridge Electronic Design). The analog EMG signal was rectified and integrated. To quantify the magnitude of the VMR at each distension pressure, the area under the curve (AUC) during the distension (20 s) was corrected for the baseline activity (AUC pre-distension, 20 s). Colonic compliance was assessed by applying

graded volumes (40-200 µl, 20 s duration) to the balloon in awake mice, while recording the corresponding colorectal pressure, as described (6, 7).

Dissociation and transfection of DRG neurons for signaling and trafficking studies. DRG were collected from C57BL/6 mice and Sprague-Dawley rats (all levels). DRG were incubated with collagenase IV (2 mg/ml) and dispase II (1 mg/ml) for 30 min (mice) and 45 min (rats) at 37°C. DRG were dispersed by trituration with a fire-polished Pasteur pipette. Dissociated neurons were transfected with $mPAR_2$-GFP (1 µg), the FRET biosensors CytoEKAR, NucEKAR, pmCKAR or CytoCKAR (all 1 µg), or with the BRET biosensors PAR_2-RLuc8 (125 ng) and βARR2-YFP (475 ng) using the Lonza 4D-Nucleofector X unit according to the manufacturer's instructions. Neurons were plated on laminin- (0.004 mg/ml) and poly-L-lysine- (0.1 mg/ml) coated glass coverslips for confocal microscopy and $[Ca^{2+}]_i$ assays, on ViewPlate-96 plates (PerkinElmer) for FRET assays, or on CulturPlates (PerkinElmer) for BRET assays. Neurons were maintained in Dulbecco's modified Eagle medium (DMEM) containing 10% fetal bovine serum (FBS), antibiotic-antimitotic, and N1 supplement for 48 h before study.

PAR_2 trafficking in DRG neurons. Mouse DRG neurons expressing $mPAR_2$-GFP were incubated with trypsin (10 nM), CS (100 nM), NE (100 nM) or vehicle (30 min, 37°C), and then fixed (4% paraformaldehyde, 20 min, 4°C). NeuN was detected by indirect immunofluorescence as described (3). Neurons were observed using a Leica SP8 confocal microscope with a HCX PL APO 63x (NA 1.40) oil objective. PAR_2 internalization in NeuN-positive neurons was quantified using ImageJ software. The border of the cytoplasm in the neuronal soma was defined by NeuN fluorescence. $mPAR_2$-GFP fluorescence within 0.5 µm of the border was defined as plasma membrane-associated receptor. The ratio of plasma membrane to cytosolic $mPAR_2$-GFP was determined (3).

FRET assays in DRG neurons. Rat DRG neurons expressing FRET biosensors were serum-restricted (0.5% FBS overnight), and equilibrated in HBSS-HEPES (10 mM HEPES, pH 7.4, 30 min, 37°C). FRET was analyzed using an Operetta CLS High-Content Imaging System (PerkinElmer) or an INCell Analyzer 2000 (GE Healthcare Life Sciences) (8-10). For CFP/YFP emission ratio analysis, cells were sequentially excited using a CFP filter (410-430 nm) with emission measured using YFP (520-560 nm) and CFP (460-500 nm) filters. Cells were imaged at 1 or 2 min intervals. Baseline was measured, neurons were challenged with trypsin (10 or 100 nM) or vehicle, and responses recorded for a further 30 min. Neurons were then incubated with the positive controls phorbol 12,13-dibutyrate (PDBu, 200 nM) for EKAR biosensors or PDBu (200 nM) plus phosphatase inhibitor cocktail-2 (SigmaAldrich, 1X, 10 min) for CKAR biosensors, and FRET was recorded for an additional 4-6 min. The use of positive controls ensured that the biosensor responses were not saturated. Data were analyzed using Harmony 4.1 or Image J 1.51 software. Images taken were aligned, cells were selected based on diameter, and fluorescence intensity was calculated for both FRET and CFP channels. Background intensity was subtracted and the FRET ratio was determined as the change in the FRET/donor (EKAR) or donor/FRET (CKAR) emission ratio relative to the baseline for each cell (F/F_0). Cells with >5% change in F/F_0 after stimulation with positive controls were selected for analysis. Neurons were incubated with I-343 (10 µM), SCH530348 (100 nM) or vehicle (0.3% DMSO) (30 min, 37°C preincubation and inclusion throughout).

BRET assays in DRG neurons. Mouse DRG neurons were equilibrated in HBSS-HEPES (30 min, 37°C), and incubated with the Renilla luciferase substrate coelenterazine h (NanoLight Technologies) (5 µM, 5 min). BRET signals were measured at 475±30 nm and 535±30 nm using

a CLARIOstar Monochronometer Microplate Reader (BMG LabTech) before and after challenge with trypsin (10 nM), NE (100 nM) or CS (100 nM) (10). The YFP/RLuc8 ratios were normalized to baseline, and data are plotted as area under the curve for the 25 min assay.

Ca^{2+} assays in DRG neurons. $[Ca^{2+}]_i$ was measured in DRG neurons from WT and *Par_2-$Na_V1.8$* mice, as described (11). Neurons were loaded with Fura-2AM (1 μM) in Ca^{2+}- and Mg^{2+}-containing DMEM (45 min, room temperature). Fluorescence of individual neurons was measured at 340 nm and 380 nm excitation and 530 nm using a Nikon Eclipse Ti microscope with 20x magnification and a Photometrics CoolSNAP camera. Data were analyzed using Nikon Ti Element Software. Cultures were first challenged with KCl (65 mM), to identify responsive neurons, and were then exposed to trypsin (100 nM). Cells ≤ 25 μm diameter were selected for analysis. For determination of the activation threshold, the magnitude of the 340/380 ratio after exposure to trypsin was compared to the baseline ratio. Neurons were considered responsive to trypsin if the 340/380 ratio was ≥ 0.1 from baseline.

Uptake of tripartite probes in DRG neurons. Mouse DRG neurons transfected with mPAR_2-GFP were incubated with Cy5-Ethyl ester (control) or Cy5-Chol (200 nM, 60 min, 37°C), and then washed in HBSS-HEPES. Neurons were transferred to a heated chamber (37 °C) in HBSS-HEPES and were observed by confocal microscopy before or after treatment with trypsin (100 nM, 15 min). Images were obtained using a Leica TCS SP8 Laser-scanning confocal microscope with a HCX PL APO 63x (NA 1.40) oil objective. Image acquisition settings were consistent for Cy5-Chol and Cy5-ethyl ester fluorescence detection.

Cell lines, transfection. HEK293 cells were cultured in DMEM supplemented with 10% (v/v) FBS (5% CO_2, 37°C). When necessary serum restriction was achieved by replacing culture medium with DMEM containing 0.5% FBS overnight. Cells were transiently transfected using polyethylenimine (PEI) (1:6 DNA:PEI).

FRET assays in HEK293 cells. HEK293 cells were transiently transfected in 10 cm dishes (~50% confluency) with Flag-PAR_2-HA (2.5 μg) and FRET biosensors CytoEKAR, NucEKAR, pmCKAR, CytoEKAR, pmEpac or CytoEpac (2.5 μg) (8, 10). In experiments examining the role of dynamin, cells were transfected with FLAG-PAR_2-HA (1.25 μg), FRET biosensor (1.25 μg) and either DynWT-HA, DynK44E-HA or pcDNA3.1 (2.5 μg). At 24 h after transfection, cells were seeded on ViewPlate-96 well plates (PerkinElmer). FRET was assessed 72 h post-transfection, following overnight serum restriction. Cells were equilibrated in HBSS-HEPES (30 min, 37°C). FRET was measured using a PHERAstar FSX Microplate Reader (BMG LabTech). For CFP/YFP emission ratio analysis, cells were sequentially excited using a CFP filter (425/10 nm) with emission measured using YFP (550/50 nm) and CFP (490/20 nm) filters. FRET was measured before and after stimulation with trypsin (10 nM), NE (100 nM), CS (100 nM), or vehicle. To ensure that the biosensor responses were not saturated, cells were also stimulated with positive controls: PDBu (1 μM) for EKAR biosensors, PDBu (200 nM) + phosphatase inhibitor cocktail-2 (1X) for CKAR biosensors, or forskolin (10 μM) + 3-isobutyl-1-methylxanthine (100 μM) for Epac biosensors. FRET ratios (donor/acceptor intensity for EKAR, or acceptor/donor intensity for CKAR and Epac) were calculated and corrected to baseline and vehicle treatments to determine ligand-induced FRET (ΔFRET). Treatment effects were determined by comparison of area under the curve values. Signaling inhibitors were dissolved in HBSS-HEPES. PS2 and PS2 inact were dissolved in HBSS-HEPES + 1% DMSO. Cells were incubated with UBO-QIC (100 nM), AG1478 (1 μM), Gö6983 (1 μM), PS2 or PS2 inact (30 μM) or vehicle (30 min preincubation, inclusion throughout).

BRET assays in HEK293 cells. HEK293 cells were transiently transfected in 10 cm dishes (~50% confluency) with: PAR_2-RLuc8 (1 µg) and either RIT-Venus or Rab5a-Venus (both 4 µg); Flag-PAR_2-HA (1 µg) and βARR1-RLuc8 (1 µg) plus Rab5a-Venus (4 µg); or Flag-PAR_2-HA (1 µg) and $G\alpha_q$-RLuc8 (0.5 µg), Gβ (1 µg), Gγ (1 µg) and Rab5a-Venus (4 µg). To examine the role of dynamin, cells were transfected with PAR_2-RLuc8 (0.5 µg), RIT-Venus or Rab5a-Venus (2 µg), and DynWT-HA, DynK44E-HA or pcDNA3.1 (2.5 µg). At 24 h after transfection, cells were seeded on CulturPlates (PerkinElmer). The following day, cells were equilibrated in HBSS-HEPES and incubated with coelenterazine h (NanoLight Technologies) (5 µM, 5 min). RLuc8 and YFP intensities were measured at 475±30 nm and 535±30 nm, respectively, using a LUMIstar Omega Microplate Reader (BMG LabTech) before and after challenge with proteases, biopsy supernatants or vehicle. Data are presented as ligand-induced BRET, calculated as the ratio of YFP to RLuc8 signals normalized to the baseline average, followed by vehicle subtraction. Treatment effects were determined by comparison of area under the curve values.

Immunofluorescence and Structured Illumination Microscopy. HEK293 cells transiently expressing Flag-PAR_2-HA were seeded on poly-D-lysine-coated high tolerance cover-glass and incubated overnight. Cells were incubated with trypsin (10 nM) or vehicle in DMEM for 30 min at 37°C. Cells were fixed in 4% paraformaldehyde on ice for 20 min and washed in PBS. Cells were blocked for 1 h at room temperature in PBS + 0.3% saponin + 3% NHS. Cells were incubated with primary antibodies to HA (rat anti-HA, 1:1,000, Roche), EEA-1 (rabbit anti-EEA-1 1:100, Abcam), $G\alpha_q$ (mouse anti-GNAQ 1:100, Millipore) in PBS + 0.3% saponin + 1% NHS overnight at 4°C. Cells were washed in PBS and incubated with secondary antibodies (goat anti-Rat Alexa568, donkey anti-rabbit Alexa488, goat anti-mouse Dylight405, 1:1,000, Invitrogen) for 1 h at room temperature. Cells were washed with PBS and mounted on glass slides with prolong Diamond mounting medium (ThermoFisher). Cells were observed by super-resolution structured illumination microscopy (SIM) using a Nikon N-SIM Eclipse TiE inverted microscope with an SR Apo-TIRF100x/1.49 objective. Images were acquired in 3D-SIM mode using 405, 488, and 561 nm lasers and filter sets for standard blue, green, and red emission on an Andor iXon 3 EMCCD camera. Z-stacks were collected with a 125 nm z interval. NIS-Elements AR Software was used to reconstruct SIM images.

cDNAs. BRET sensors for PAR_2-RLuc8, KRas-Venus, Rab5a-Venus, βARR2-YFP, βARR2-RLuc8 and Gαq-RLuc8 have been described (3, 10). FRET sensors CytoEKAR, NucEKAR, CytoCKAR and pmCKAR (8) were from Addgene (plasmids 18680, 18681, 14870, 14862, respectively).

IP_1 accumulation assay. KNRK-hPAR_2, KNRK, HEK293, or HT-29 cells were seeded at a density of $50x10^3$ cells/well onto clear 96-well plates (PerkinElmer). After 24 h of culture, medium was replaced with IP_1 stimulation buffer (10 mM HEPES, 1 mM $CaCl_2$, 0.5 mM $MgCl_2$, 4.2 mM KCl, 146 mM NaCl, 5.5 mM glucose, 50 mM LiCl; 37°C, 5% CO_2). Cells were pre-incubated with the antagonist or vehicle for 30 min prior to the addition of agonist. Cells were then further incubated for 40 min. Stimulation buffer was aspirated and the cells were incubated in lysis buffer for 10 min (IP-One HTRF® assay kit, Cisbio). Lysates were transferred to a 384-well OptiPlate (PerkinElmer), and IP_1 was detected (IP-One HTRF® assay kit, Cisbio). Homogeneous time resolved FRET was measured with an Envision plate reader (PerkinElmer Life Sciences).

Synthesis of I-343, MIPS15479, Cy5-cholestanol, Cy5-ethyl ester. Reagents were from Chem-Impex, Aldrich and Novabiochem. ^1H NMR spectra were obtained using a Bruker Advance DPX

300 spectrometer at 300.13 MHz, or a Varian Unity Inova 600 spectrometer at 599.8 MHz. ^{13}C NMR spectra were obtained using a Varian Unity Inova 600 spectrometer at 150.8 MHz, or on a Bruker Avance DPX 300 spectrometer at 75.4 MHz. Unless stated otherwise, samples were dissolved in $CDCl_3$. Thin-layer chromatography used 0.2 mm plates and Merck silica gel 60 F254. Column chromatography used Merck silica gel 60 (particle size 0.063-0.200 μm, 70- 230 mesh). High resolution mass spectra (HR-ESI) were obtained using a Waters LCT Premier XE (TOF) with electrospray ionization. Compound purity was analyzed via LCMS (Agilent 1200 series LC coupled directly to a photodiode array detector and an Agilent 6120 Quadrupole MS) using a Phenomenex column (Luna 5 μm C8, 50 mm 4.60 mm ID). All compounds were of >95% purity.

I-343. 5-methyl-1*H*-1,2,4-triazole-3-carboxylic acid (1.2 eq) was dissolved in DMSO, and then mixed with HATU (1.2 eq), the corresponding amine (1.0 eq), and DIPEA (2.5 eq) (RT, overnight). Water was added and the solids were filtered and washed to generate the product (88% yield). ^1H NMR (400 MHz, DMSO) δ 8.52 (d, J = 7.2 Hz, 1H), 8.18 – 8.10 (m, 2H), 7.48 (d, J = 8.8 Hz, 1H), 7.45 – 7.36 (m, 2H), 4.34 – 3.66 (m, 6H), 2.43 – 2.30 (m, 3H), 1.61 (s, 6H), 1.56 (s, 3H), 1.54 (s, 3H), 1.48 (s, 3H). LCMS: Rf =3.37, m/z = 519.3 ($M+H^+$).

MIPS15479. Sodium azide (5 mmol) and tert-butyl bromoacetate (5 mmol) were mixed with DMF (10 ml) (RT, 72 h). Propiolic acid (5 mmol) and CuI (0.5 mmol) were added and the stirring continued (RT, 48 h). The reaction mixture was adjusted to pH4 with 1N HCl, and the resultant mixture poured into brine. The aqueous phase was extracted with DCM, dried over $MgSO_4$, and evaporated to dryness. The crude residue was purified on silica gel to generate the product (29.5% yield). ^1H NMR (401 MHz, DMSO) δ 8.76 – 7.63 (m, 2H), 5.42 – 5.19 (m, 2H), 1.43 (s, 9H). LCMS: Rf = 2.90, m/z = 225.9 (M-H, $C_9H_{12}N_3O_4^-$). The triazole acid (1.1 eq), the amine HCl salt (from WO 2015048245 patent; 1.0 equivalent) and DIPEA (2.5 to 3.5 eq) were dissolved in DMF. PyOxim (1.25 eq) was added and the mixture was stirred (RT, overnight). Water and EtOAc were added and the phases separated. The organic phase was washed 2 times with 1N HCl and then saturated bicarbonate solution. The aqueous phase was back extracted with more EtOAc. All EtOAc phases were combined, dried over $MgSO_4$, filtered, and evaporated under reduced pressure. The product was purified on silica gel to generate the ester, which was deprotected with TFA and DCM (1:1) to provide the product (95% yield). LCMS: Rf = 3.56, m/z = 562.9 (M+H, $C_{28}H_{32}FN_8O_4^+$) (ester intermediate, ^1H NMR (401 MHz, $CDCl_3$) δ 8.37 (s, 1H), 8.27 (d, J = 5.8 Hz, 1H), 7.93 (dd, J = 8.8, 5.3 Hz, 2H), 7.24 (d, J = 4.1 Hz, 1H), 7.19 (t, J = 8.6 Hz, 2H), 5.13 – 5.07 (m, 2H), 4.60 – 4.44 (m, 4H), 3.96 – 3.89 (m, 2H), 1.70 (s, 2H), 1.66 (s, 4H), 1.63 – 1.58 (m, 9H), 1.49 – 1.47 (m, 9H). LCMS: Rf = 3.71, m/z = 619.0 (M+H, $C_{32}H_{40}FN_8O_4^+$). The spacer-lipid conjugate (NH_2-PEG_{12}-Asp(OChol)-resin) was prepared by manual peptide synthesis with standard Fmoc chemistry on NovaSyn®TG^R R resin (loading 0.18 mmol/g). Coupling of the Fmoc-Asp(OChol)-OH (1.5 eq) with (1H-Benzotriazol-1-yloxy)(tri-1-pyrrolidinyl)phosphonium hexafluorophosphate (PyBOP, 2 eq) in dichloromethane (DCM) with activation *in situ* was accomplished using diisopropylethylamine (DIPEA, 3 eq) for 3 h. Fmoc deprotection was achieved using 20% piperidine in *N*,*N*-dimethylformamide (DMF). Fmoc-PEG_{12}-OH (2 eq) was coupled to resin-bound NH_2-Asp(OChol) with PyBOP (2 eq) and DIPEA (3 eq) in DCM. Fmoc deprotection was achieved using 20% piperidine in *N*,*N*-dimethylformamide (DMF). Following final deprotection, the antagonists were coupled to the spacer-lipid conjugate on resin. The triazole acetic acid (2-3eq) was coupled to resin-bound NH_2-PEG_{12}-Asp(OChol)-resin (250 mg) with PyBOP (2 eq) and DIPEA (3 eq) in DCM overnight. The construct was then cleaved from resin using 95% trifluoroacetic acid and purified by reverse-phase high-performance liquid chromatography (HPLC) (Phenomenex Luna C8 column) with 0.1% TFA/H_2O and 0.1% TFA/ACN as solvents, providing the lipidated antagonists as viscous oils (45% yield). ^1H NMR (401 MHz, $CDCl_3$) δ 8.43 (d, J = 4.2 Hz, 2H), 7.99 – 7.90 (m, 2H), 7.74 – 7.50 (m, 3H), 7.34 – 7.26 (m, 2H), 7.19 (dt, J = 19.6, 7.5 Hz, 3H), 5.22 (s, 2H), 4.95 – 4.86 (m, 1H), 4.74 – 4.64 (m,

1H), 4.62 – 4.40 (m, 4H), 4.28 – 4.17 (m, 1H), 3.97 – 3.79 (m, 3H), 3.74 – 3.54 (m, 45H), 3.49 (dd, *J* = 10.9, 5.7 Hz, 2H), 3.03 (dd, *J* = 17.2, 5.1 Hz, 1H), 2.70 (dd, *J* = 17.9, 5.9 Hz, 1H), 2.57 (t, *J* = 3.8 Hz, 2H), 1.96 (dd, *J* = 9.3, 3.1 Hz, 1H), 1.86 – 1.18 (m, 43H), 1.18 – 0.78 (m, 26H), 0.67 – 0.58 (m, 4H). LCMS (high res): m/z = 824.5132 (M+2H, $C_{86}H_{138}FN_{11}O_{19}^{2+}$).

Cy5-cholestanol, Cy5-ethyl ester. These tripartite probes were synthesized as described (3).

Statistics. Results are mean±SEM. Differences were assessed using Student's t test (two comparisons), or one- or two-way ANOVA (multiple comparisons) followed by Tukey's multiple comparisons test (electrophysiology assays) or Dunnett's multiple comparisons test (somatic nociception, single cell FRET assays). For BRET assays and population FRET assays, area under the curve data were normalized to matched trypsin alone responses, and compared to 100% using a one-sample t-test. For assays of colonic nociception (VMR to CRD), data were statistically analyzed by generalized estimating equations followed by Fisher's Least Significant Difference post-hoc test when appropriate using SPSS 23.0. GraphPad Prism 7 Software (San Diego, CA, USA) was used for statistical analysis and preparation of graphs.

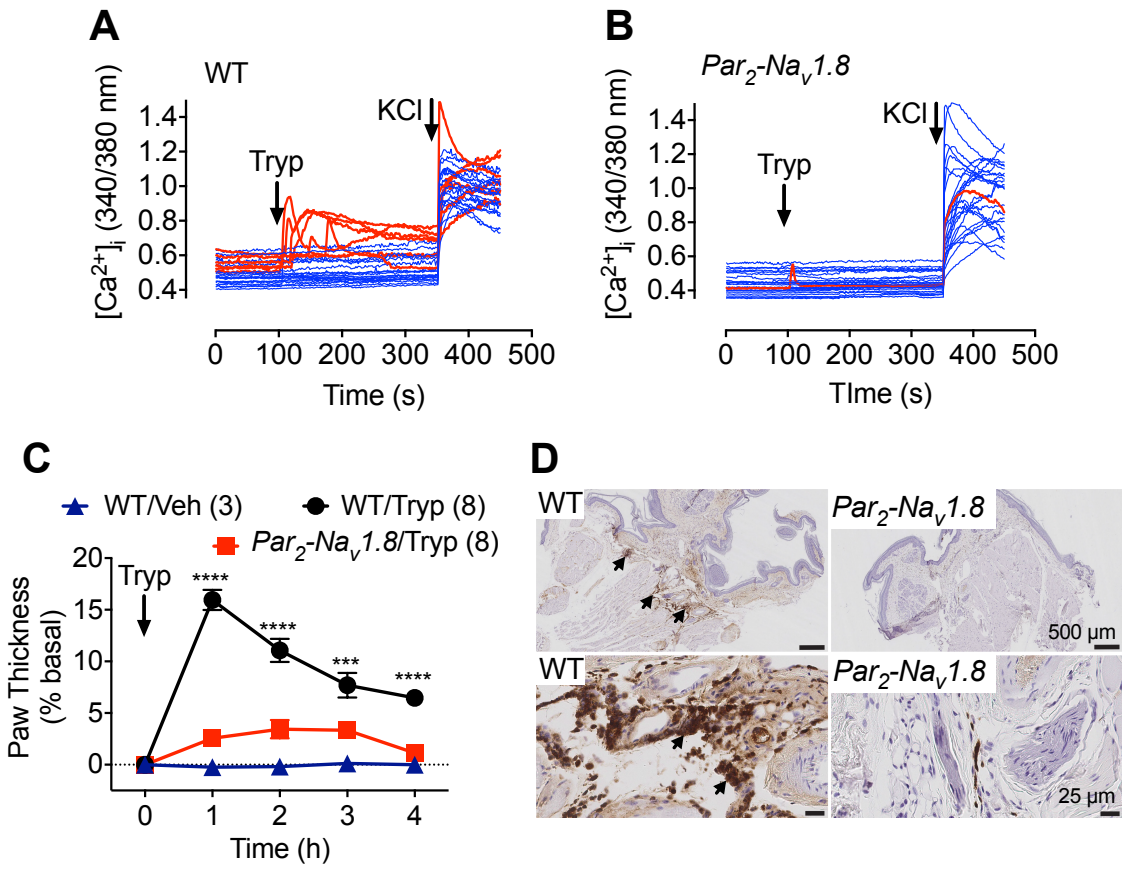

Fig. S1. Expression of functional PAR_2 in DRG neurons, and PAR_2-dependent inflammation. A, B. Representative traces of effects of trypsin (100 nM) on $[Ca^{2+}]_i$ in DRG neurons from WT (**A**) and *Par₂-Na$_V$1.8* (**B**) mice. Traces from 25 neurons are shown; traces from trypsin-responsive neurons are shown in red. In WT mice, 20/65 (31%) of neurons responded to trypsin. In *Par₂-Na$_V$1.8* mice, 3/51 (6%) of neurons responded to trypsin. Neurons were collected from 4 mice per group. **C.** Effect of intraplantar injection of trypsin on paw thickness in WT and *Par₂-Na$_V$1.8* mice. ***P<0.001, ****P<0.0001. Numbers in parentheses denote mouse numbers. **D.** Effect of intraplantar injection of trypsin on neutrophil infiltration into the paw at 4 h in WT and *Par₂-Na$_V$1.8* mice. Arrows show neutrophil influx in WT mice.

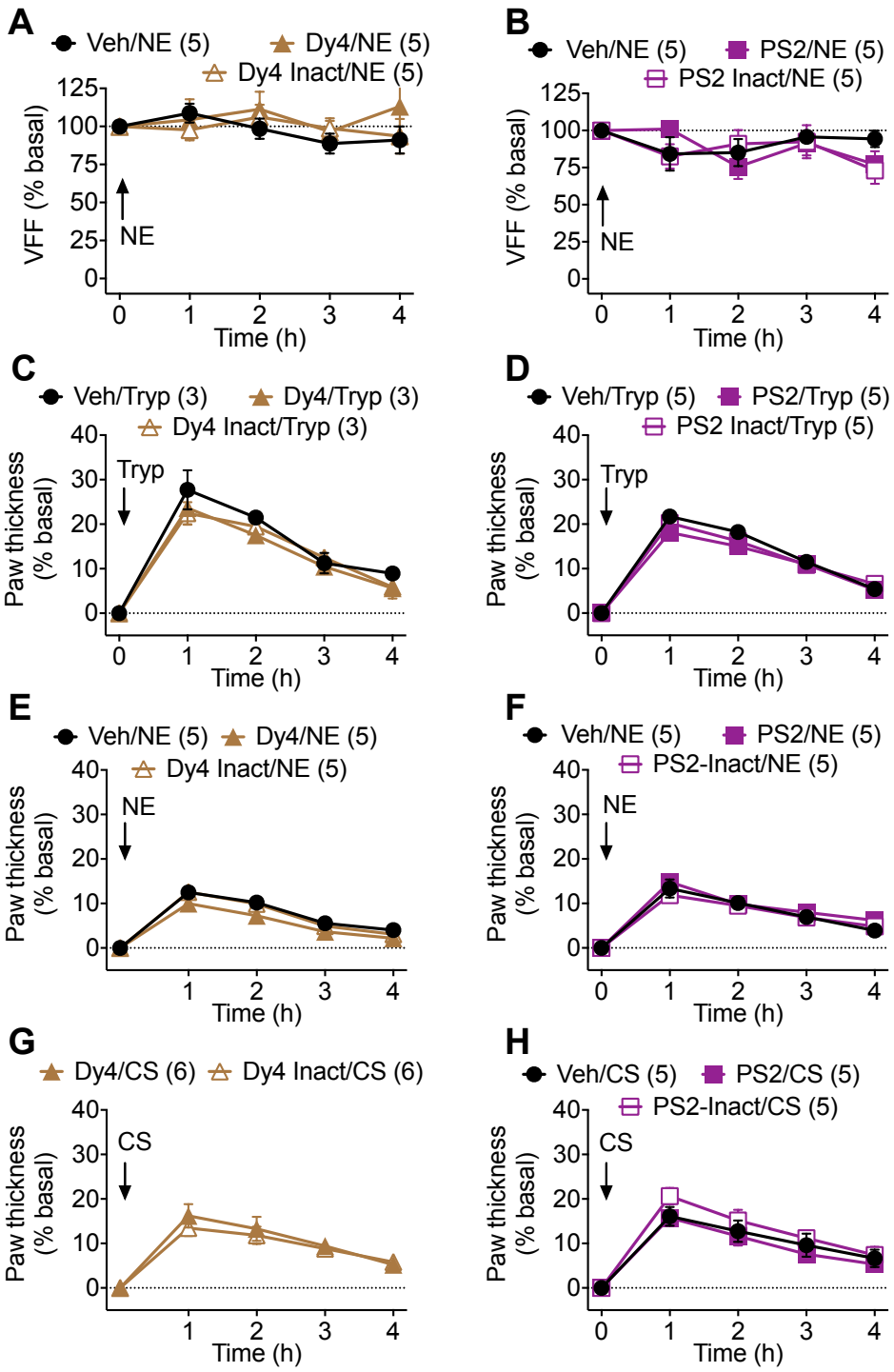

Fig. S2. Protease-induced mechanical nociception and edema. A, B. VFF withdrawal responses of the contralateral (right) paw after intraplantar injections into the ipsilateral (left) paw of Dy4 or Dy4 inact (**A**), PS2 or PS2 inact (**B**), or vehicle (Veh), followed by NE. **C-H.** Thickness of the ipsilateral paw. Dy4 or Dy4 inact (**C, E, G**), PS2 or PS2 inact (**D, F, H**), or vehicle (Veh) was administered by intraplantar injection into mouse paw. After 30 min, trypsin (Tryp) (**C, D**), NE (**E, F**) or CS (**G, H**) was injected. Paw thickness (edema) was measured. Numbers in parentheses denote mouse numbers.

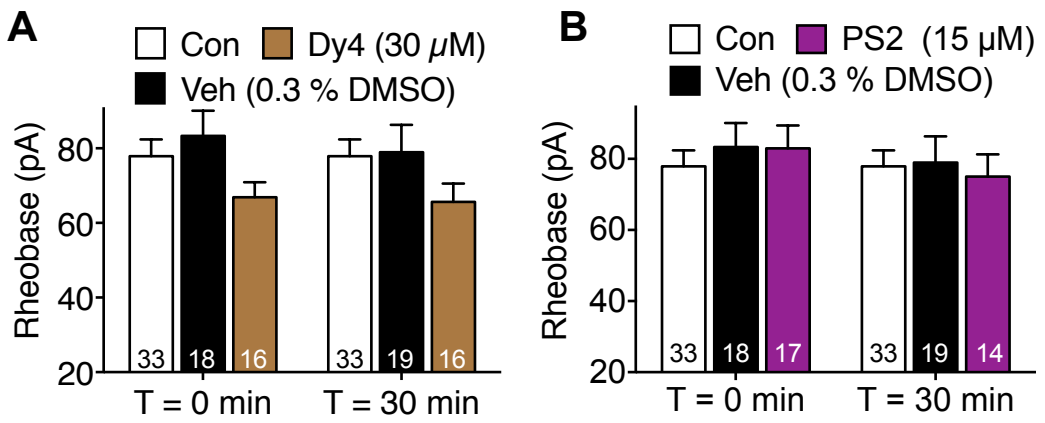

Fig. S3. Endocytic inhibitors and baseline hyperexcitability of nociceptors. Rheobase of mouse DRG neurons preincubated with buffer control (Con), vehicle (Veh, 0.3% DMSO), Dy4 (**A**) or PS2 (**B**). Rheobase was measured at T 0 min or T 30 min after washing. Numbers in bars denote neuron numbers.

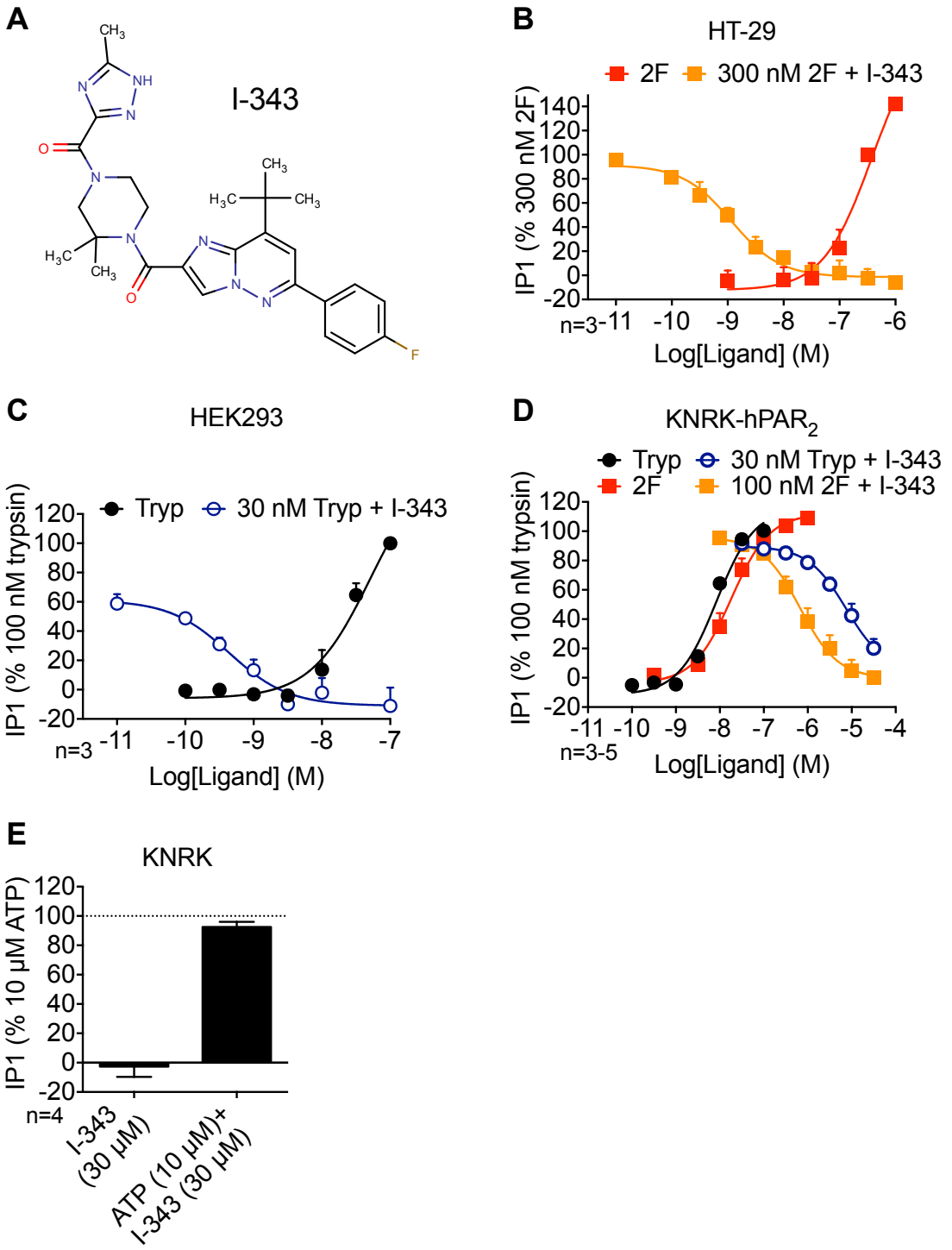

Fig. S4. Characterization of PAR_2 antagonist I-343. A. I-343 structure. **B-D.** Concentration-response analysis of the effects of I-343 on 2F- and trypsin-induced IP_1 accumulation in HT-29 (**B**), HEK293 (**C**) and KNRK-hPAR_2 (**D**) cells. **E.** Effects of I-343 on ATP-induced IP_1 accumulation in HEK cells. n, experimental replicates from triplicate observations.

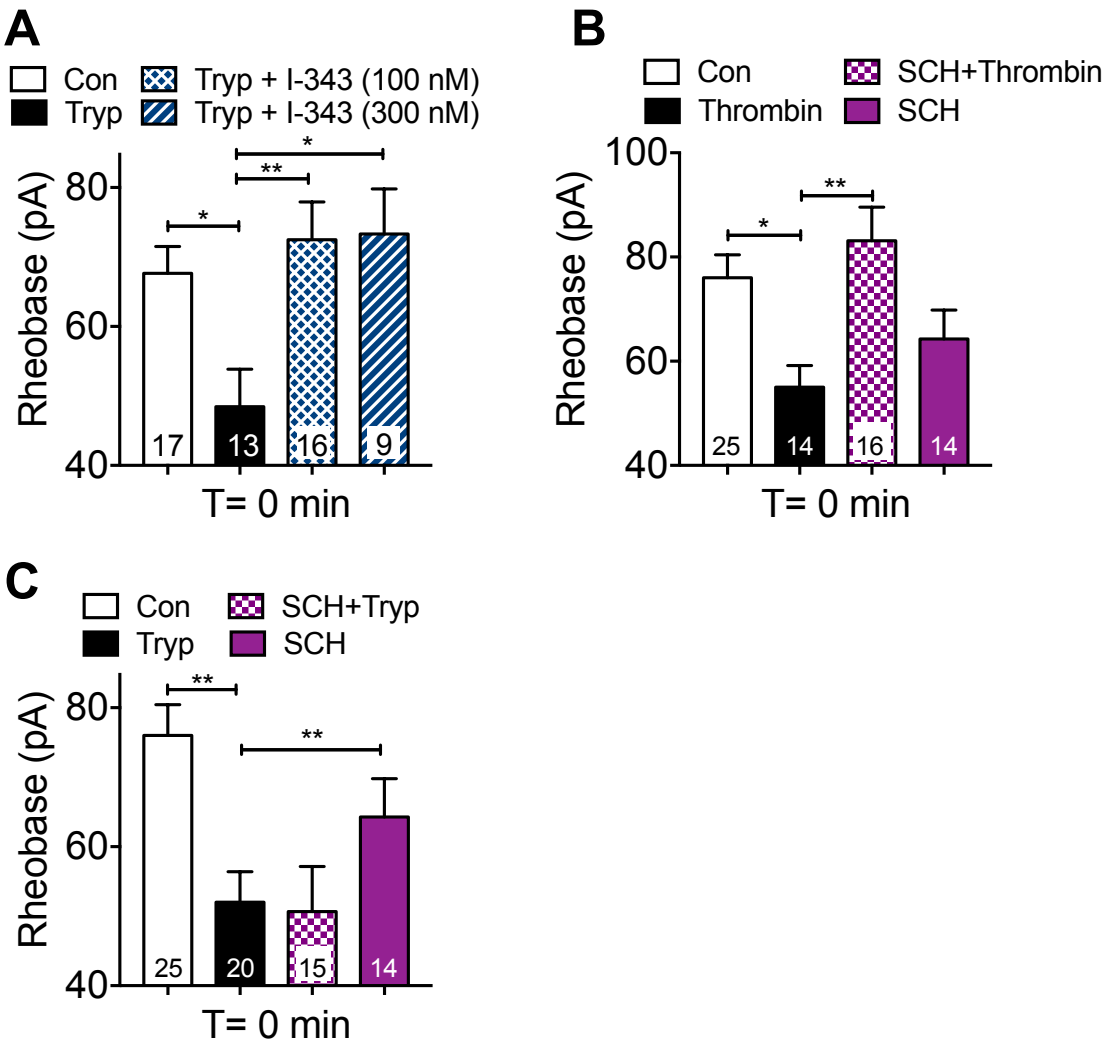

Fig. S5. Trypsin- and thrombin-induced hyperexcitability of nociceptors. Rheobase of mouse DRG neurons preincubated with I-343 (**A**, PAR_2 antagonist) or SCH79797 (**B, C**, PAR_1 antagonist). Neurons were challenged with trypsin (**A, C**) or thrombin (**B**), washed, and rheobase was measured 0 min later. **P*<0.05, ***P*<0.01. Numbers in bars denote neuron numbers.

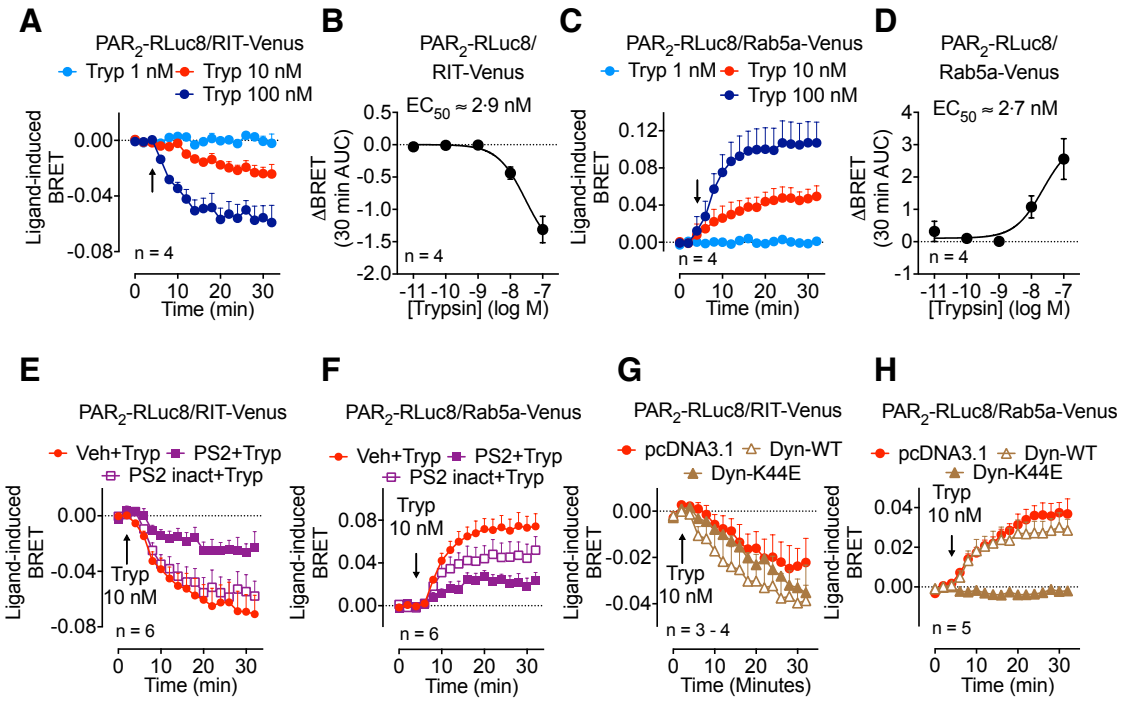

Fig. S6. PAR_2 endocytosis in HEK293 cells. PAR_2-RLuc8/RIT-Venus BRET (**A, B, E, G**) and PAR_2-RLuc8/Rab5a-Venus BRET (**C, D, F, H**) in HEK293 cells. n, experimental replicates from triplicate observations.

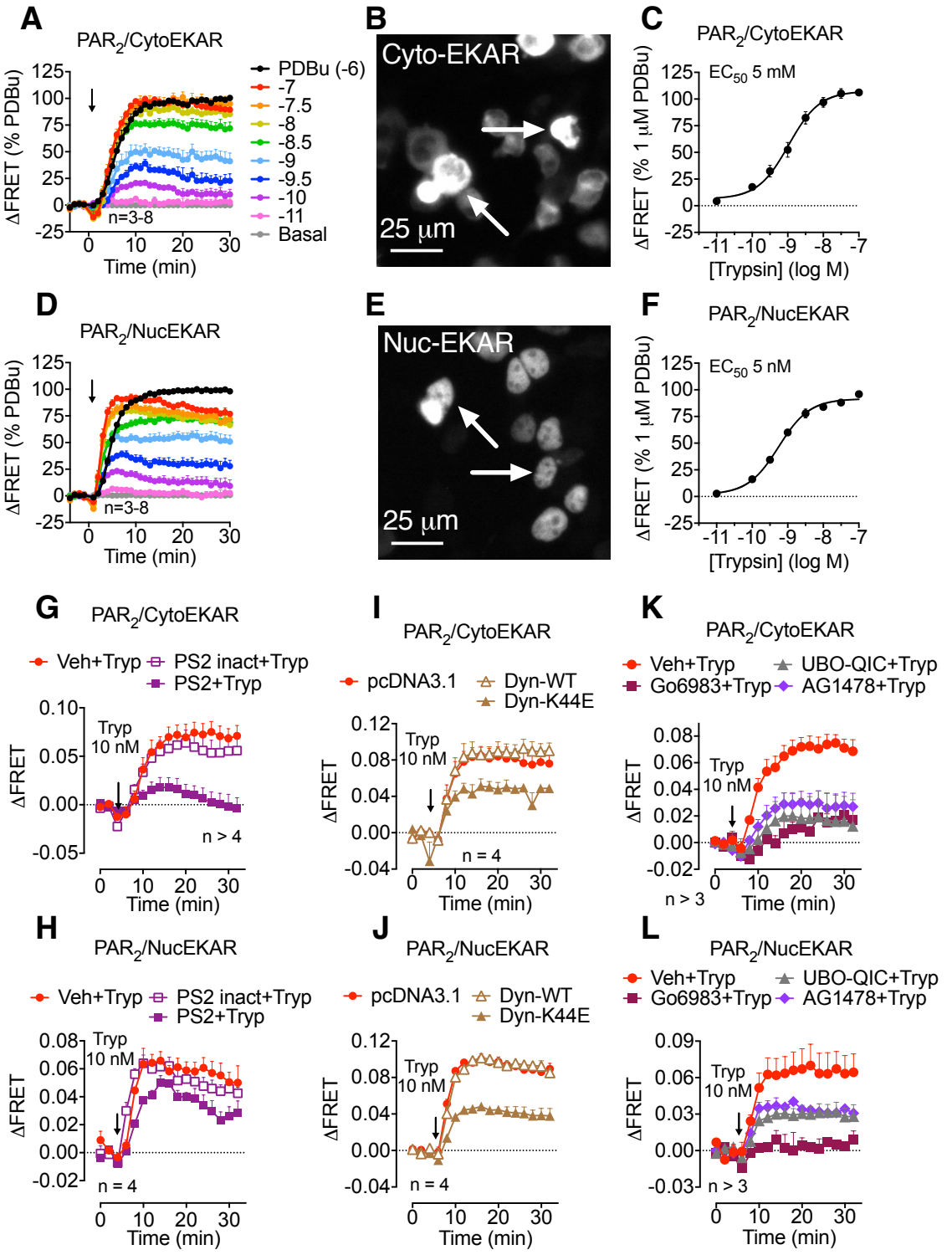

Fig. S7. PAR$_2$ compartmentalized ERK signaling in HEK293 cells. FRET assays of cytosolic (**A-C, G, I, K**) and nuclear (**D-F, H, J, L**) ERK activity in HEK293 cells. **B, E.** Sensor localization. n, experimental replicates from triplicate observations.

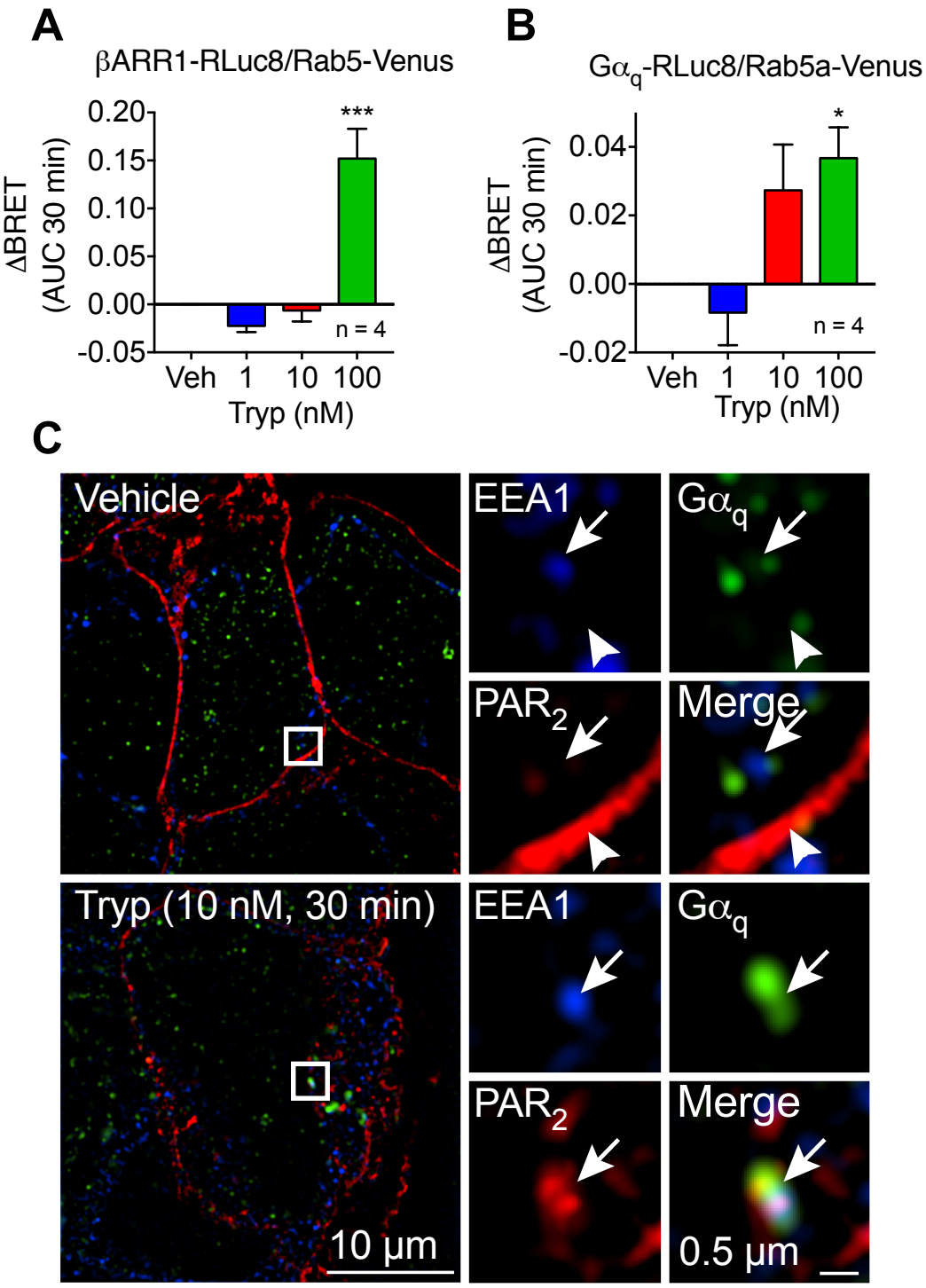

Fig. S8. Trafficking of PAR_2, βARR1 and $G\alpha_q$ to early endosomes in HEK293 cells. A, B. βARR1-RLuc8/Rab5a-Venus BRET (**A**) and $G\alpha_q$-RLuc8/Rab5a-Venus BRET (**B**) in HEK293 cells. **P*<0.05, ****P*<0.001 compared to vehicle. n, experimental replicates from triplicate observations. **C.** Localization of EEA1, $G\alpha_q$, and PAR_2 in endosomes after treatment with vehicle or trypsin for 30 min. Arrow heads show colocalization of EEA1, $G\alpha_q$, and PAR_2 in endosomes of trypsin-treated cells.

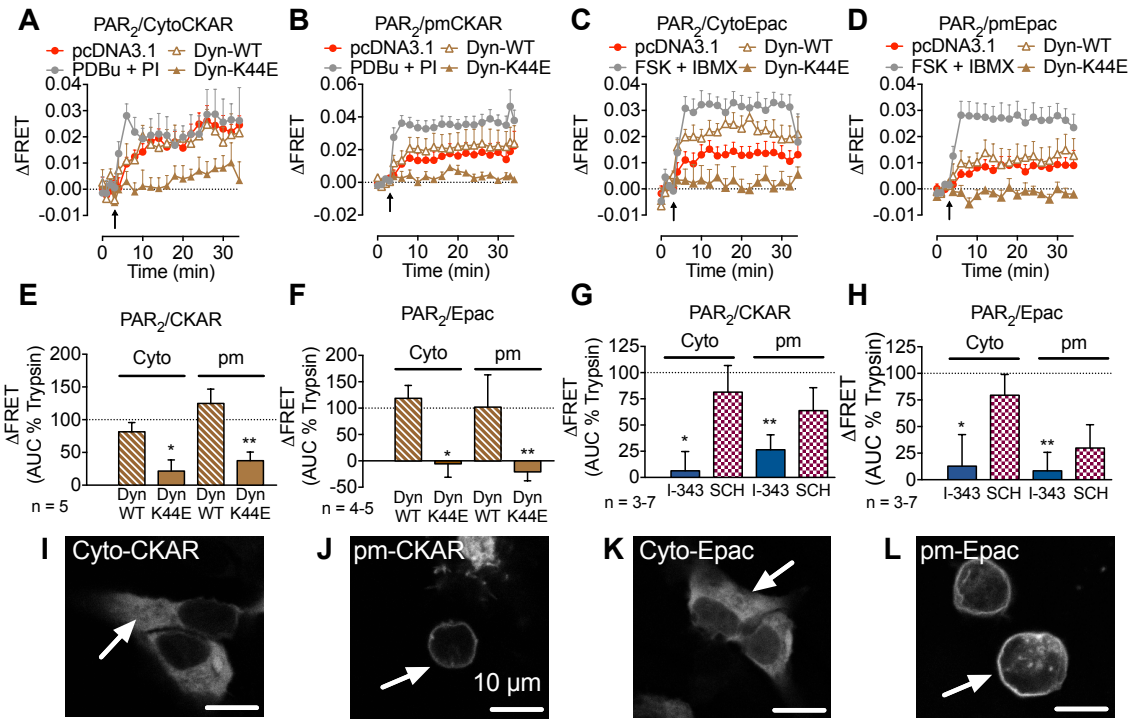

Fig. S9. PAR_2 compartmentalized PKC and cAMP signaling in HEK293 cells. FRET assays of cytosolic PKC (**A, E, G**), plasma membrane PKC (**B, E, G**), cytosolic cAMP (**C, F, H**) and plasma membrane cAMP (**D, F, H**) in HEK293 cells. **I-L.** Sensor localization. AUC, area under curve. **P*<0.05, ***P*<0.01 compared to control. n, experimental replicates, triplicate observations.

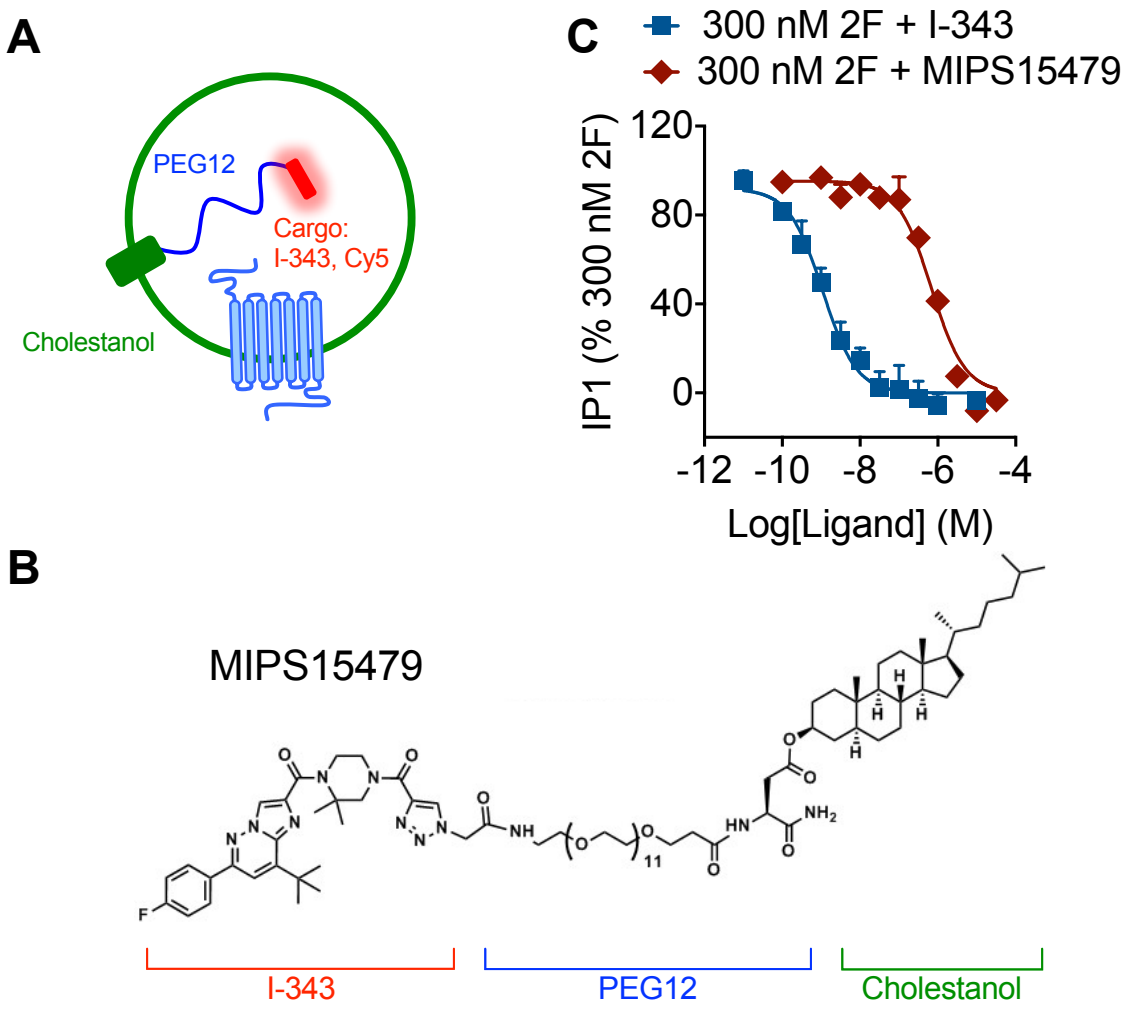

Fig. S10. Tripartite PAR_2 antagonist. A. Principal of targeting PAR_2 in endosomes using a tripartite probe. **B.** Structure of MIPS15479 tripartite PAR_2 antagonist. **C.** Concentration-response analysis of the effects of I-343 and MIPS15479 on 2F-induced IP_1 accumulation in HT-29 cells.

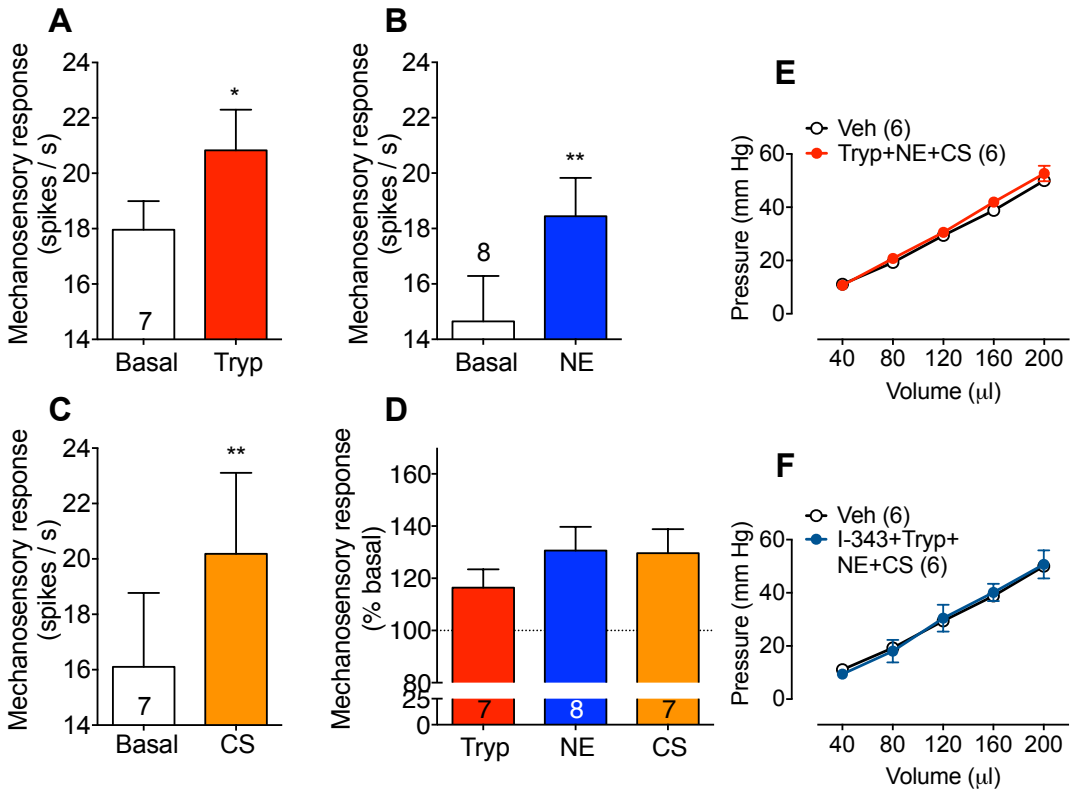

Figure S11. Sensitization of colonic afferents and colonic compliance. A-D. Mechanosensory responses of mice measured 28 d after exposure to TNBS. The colonic mucosa was stimulated with a 2 g VFF under basal conditions and after exposure of receptive fields to trypsin (**A, D**, Tryp), NE (**B, D**) or CS (**C, D**). **D.** Responses as % basal. Numbers in bars denote afferent numbers. **E, F.** Colonic compliance in awake healthy control mice. Pressure/volume relationships were unchanged by a protease cocktail (**E**) or by I-343 (**F**), which indicates that compliance of the colon is unchanged. Numbers in parentheses denote mouse numbers. **P*<0.05, ***P*<0.01.

Movie S1. Targeting PAR_2 in endosomes of nociceptors. The movie shows trafficking of endosomes containing $mPAR_2$-GFP and Cy5-Chol in neurites of mouse DRG neurons. Neurons were incubated with Cy5-Chol, washed and recovered for 3 h. Neurons were then challenged with trypsin for 15 min, and imaged.

Movie S2. Mechanisms of protease- and PAR_2-induced hyperexcitability of nociceptors. The movie illustrates mechanisms by which trypsin, NE and CS induce PAR_2-dependent hyperexcitability of nociceptors.

References

1. Valdez-Morales EE*, et al.* (2013) Sensitization of peripheral sensory nerves by mediators from colonic biopsies of diarrhea-predominant irritable bowel syndrome patients: a role for PAR2. *Am J Gastroenterol* 108(10):1634-1643.
2. Stirling LC*, et al.* (2005) Nociceptor-specific gene deletion using heterozygous NaV1.8-Cre recombinase mice. *Pain* 113(1-2):27-36.
3. Jensen DD*, et al.* (2017) Neurokinin 1 receptor signaling in endosomes mediates sustained nociception and is a viable therapeutic target for prolonged pain relief. *Sci Transl Med* 9(392).
4. Brierley SM, Jones RC, 3rd, Gebhart GF, & Blackshaw LA (2004) Splanchnic and pelvic mechanosensory afferents signal different qualities of colonic stimuli in mice. *Gastroenterology* 127(1):166-178.
5. Hughes PA*, et al.* (2009) Post-inflammatory colonic afferent sensitisation: different subtypes, different pathways and different time courses. *Gut* 58(10):1333-1341.
6. Castro J*, et al.* (2017) Cyclic analogues of alpha-conotoxin Vc1.1 inhibit colonic nociceptors and provide analgesia in a mouse model of chronic abdominal pain. *Br J Pharmacol* 10.1111/bph.14115.
7. Vermeulen W*, et al.* (2013) Role of TRPV1 and TRPA1 in visceral hypersensitivity to colorectal distension during experimental colitis in rats. *Eur J Pharmacol* 698(1-3):404-412.
8. Halls ML, Poole DP, Ellisdon AM, Nowell CJ, & Canals M (2015) Detection and Quantification of Intracellular Signaling Using FRET-Based Biosensors and High Content Imaging. *Methods Mol Biol* 1335:131-161.
9. Jensen DD*, et al.* (2014) Endothelin-converting Enzyme 1 and beta-Arrestins Exert Spatiotemporal Control of Substance P-induced Inflammatory Signals. *J Biol Chem* 289(29):20283-20294.
10. Yarwood RE*, et al.* (2017) Endosomal signaling of the receptor for calcitonin gene-related peptide mediates pain transmission. *Proc Natl Acad Sci USA* 114(46):12309-12314.
11. Ono K*, et al.* (2017) Cutaneous pigmentation modulates skin sensitivity via tyrosinase-dependent dopaminergic signalling. *Sci Rep* 7(1):9181.